

Interference and Interaction in multi-wall carbon nanotubes

C. Schönenberger¹, A. Bachtold¹, C. Strunk¹, J.-P. Salvetat², L. Forró²

¹Institut für Physik, Universität Basel, Klingelbergstr. 82, CH-4056 Basel, Switzerland

²Institut de Génie Atomique, École Polytechnique Fédérale de Lausanne, CH-1015 Lausanne, Switzerland

Received: 17 May 1999/Accepted: 18 May 1999/Published online: 4 August 1999

Abstract. We report equilibrium electric resistance R and tunneling spectroscopy (dI/dV) measurements obtained on single multi-wall nanotubes contacted by four metallic Au fingers from above. At low temperature quantum interference phenomena dominate the magnetoresistance. The phase-coherence (l_ϕ) and elastic-scattering lengths (l_e) are deduced. Because l_e is of order of the circumference of the nanotubes, transport is quasi-ballistic. This result is supported by a dI/dV spectrum which is in good agreement with the density of states (DOS) due to the one-dimensional subbands expected for a perfect single-wall tube. As a function of temperature T the resistance increases on decreasing T and saturates at $\approx 1\text{--}10$ K for all measured nanotubes. $R(T)$ cannot be related to the energy-dependent DOS of graphene but is mainly caused by interaction and interference effects. On a relatively small voltage scale of the order ≈ 10 meV, a pseudogap is observed in dI/dV which agrees with Luttinger-liquid theories for nanotubes. Because we have used quantum diffusion based on Fermi-liquid as well as Luttinger-liquid theory in trying to understand our results, a large fraction of this paper is devoted to a careful discussion of all our results.

PACS: 73.61.Wp; 72.15.Gd; 73.20.Fz; 73.20.At

In recent years carbon nanotubes have surprised us with remarkable properties which are neither present in graphite nor in diamond [1]. Nanotubes are ideal model systems for the investigation of low-dimensional molecular conductors whose electronic properties are largely determined by molecular orbitals that are extended along the whole conductor similar to metals. The length-to-diameter ratio can exceed 10^5 for the smallest diameter tubes ($\gtrsim 100$ μm in length and ≈ 1 nm in diameter). A carbon nanotube is obtained from a slice of graphene sheet wrapped into a seamless cylinder. Depending on the specific realization (the wrapping vector), the nanotube may be a true one-dimensional metal with a non-vanishing density of states at the Fermi energy or a semiconductor with a gap. This is in marked contrast to the two-dimensional

graphene sheet which is a zero-gap semiconductor. By combining metallic and semiconducting tubes, either in their intrinsic or doped forms, the whole span of electronic components ranging from wires, bipolar devices to field-effect transistors may be embodied in nanotubes. A striking field-effect has already been demonstrated at room temperature [2]. On the fundamental side, a perfect metallic nanotube is supposed to be a ballistic conductor in which only two one-dimensional ($1d$) subbands (modes) carry the electric current [3]. Because of the relatively low carrier concentration as compared to ordinary metals such as Au, strong correlations due to Coulomb interactions are expected [4, 5].

Nanotubes can be fabricated in two basic forms: either as single-wall cylinders (SWNT = single-wall nanotube) or as wires that consist of a set of concentric cylinders (MWNT = multi-wall nanotube). Furthermore, both forms may be present as single wires or packed into ropes. A remarkable variety of physical phenomena have been observed in electrical transport to date. The first signature of quantum effects were found in the magnetoresistance (MR) of MWNTs. Song et al. studied bundles of MWNTs [6] while Langer et al. was able to measure the MR of a single MWNT for the first time [7]. In both cases a negative MR was observed at low temperatures indicative of weak localization. However, the phase-coherence length l_ϕ was found to be small amounting to only $\lesssim 20$ nm at 0.3 K, in strong contrast to the ballistic transport with only 2 modes theoretically expected for a perfect nanotube. Evidence for much larger coherence lengths in SWNTs was provided by the observation of zero-dimensional states in single-electron tunneling experiments [8, 9]. Recently, a pronounced Aharonov–Bohm resistance oscillation has been observed in MWNTs [10]. This experiment has provided compelling evidence that l_ϕ can exceed the circumference of the tube so that large coherence lengths are possible for MWNTs too, see also [11]. Because the magnetic-flux-modulated resistance agreed with an Aharonov–Bohm flux of $h/2e$ the effect is supposed to be caused by conventional weak-localization for which backscattering of electrons is essential. In essence, as in the work of Langer et al. [7], $2d$ -diffusive transport could explain

the main observation reasonably well. The Aharonov–Bohm experiment led to a convincing proof that the electric current flows in the outermost (metallic) graphene tube only, at least at low temperatures $T \lesssim 70$ K. Presumably, this is a consequence of the way in which the nanotubes are contacted. Electrodes are evaporated over the MWNT and therefore contact the outermost tube preferentially. Because it is only the outermost tube that carries the current, large-diameter single graphene cylinders can now be investigated. Very recently, proximity-induced superconductivity was found in weak links formed by a nanotube in contact with two superconducting banks [12].

All these striking results mentioned were obtained by contacting a single nanotube with the aid of micro- and nanostructuring technologies. Alternative approaches have been developed as well. For example, Dai et al. and Thess et al. have measured the voltage drop along nanotubes using movable tips [13] and Kasumov et al. have developed a pulsed-laser deposition method [14]. Furthermore, scanning-probe manipulation schemes were developed [15] and recently it has been shown that SWNTs can directly be synthesized to bridge pre-patterned structures [16]. Still another elegant method allowing one to electrically contact a single MWNT has been used by Frank et al. [17]. The nanotube, which is attached to a tip, is contacted by immersing it into a liquid metal such as mercury. Immersing and pulling out the nanotube repeatedly is claimed to have a cleaning effect. In particular, graphitic particles are removed from the tubes. After some repetitions, an almost universal conductance close to the quantized value $G_0 := 2e^2/h$ is measured. From these experiments the researchers conclude that transport in MWNTs is ballistic over distances of the order of $\gtrsim 1 \mu\text{m}$. This is very striking because the experiments were conducted at room temperature. At present it is not clear why the conductance is close to G_0 instead of the theoretically expected value of $2G_0$.

Our results, which were obtained on similarly arc-produced MWNTs, appear to be in strong contradiction to the ballistic transport of Frank et al. [17]. It is one aim of this paper to address this contradiction by quantifying the degree of backscattering (or diffusiveness) observed in our samples due to static disorder. As will be demonstrated, the discrepancy is much weaker than originally thought. It turns out that our nanotubes may be regarded as quasi-ballistic conductors, at least at low temperature. At room temperature the degree and source of backscattering is difficult to quantify. But because the measured resistances are in quite good agreement with theoretically predicted values backscattering must be relatively weak.

The fabrication of reliable electric contacts to single carbon nanotubes has been an issue of great attention during recent years and quite some progress has been made [8–20]. The same remark is appropriate for the quality of the nanotubes. The electric contact resistances of SWNTs and MWNTs, which were adsorbed on a prestructured electrode pattern, were found to be large, in the $\text{M}\Omega$ range [8, 11, 18]. The contact resistance can be reduced by local electron-beam irradiation enabling one to select a single nanotube for measurement [18]. If the contacts are high-ohmic, they determine the measured two-terminal resistance. Under such circumstances four-terminal measurement schemes are usually applied in order to measure the intrinsic resistance. The first four-terminal resistance measurements on single MWNTs

were realized by Ebbesen et al. [19]. All kind of temperature dependences were found. Since resistivities at 300 K varied by six orders of magnitude, from 5×10^{-6} to $6 \Omega\text{cm}$, this was taken as evidence that nanotubes can be metallic or semiconducting. However, these results suffer from possible damage caused by the method used to structure the devices (ion-induced deposition using a metalorganic precursor gas). Much lower contact resistances can be obtained if the contacts are evaporated directly onto the nanotubes. Our own record is presently at $R_c \lesssim 100 \Omega$. Note, that we define the contact resistance by $R_c = (R_{2t} - R_{4t})/2$, where R_{4t} denotes the four-terminal resistance (outer contacts are used for current source and drain, whereas the two inner ones serve to measure the voltage drop) and R_{2t} denotes the two-terminal resistance measured using only the two inner contacts.

At this point an important remark has to be made. If we assume that the nanotubes are indeed nearly perfect, for the sake of the argument, say ballistic, a quantized resistance is expected providing the contacts are ideal (no backscattering off the contacts). For the nanotube with two propagating modes the resistance would then equal $h/4e^2$. This resistance is known to be a pure contact resistance which originates from distributing the current carried by a few modes into many modes of a macroscopic reservoir [21]. Hence, once the original goal to lower apparent contact resistances (i.e. R_c) has been achieved, we end up measuring in either two- or four-terminal configuration the same quantized contact resistance [22, 23]. Because the distinction between two- and four-terminal resistance disappears for ideal contacts, one could equally well step back to the original two-terminal configuration in this situation. In reality contacts are not expected to be perfect: most importantly, the contact is abrupt and therefore everything else than an adiabatic widening which is realized in semiconductor split-gate point contacts [24]. Hence, we expect that each contact attached to a nanotube will inevitably induce some degree of backscattering. In such a realistic case, it is difficult to relate the measured resistance with either the ‘intrinsic’ resistance or the one that would be measured if the contacts were ideal. For the experiments we are going to discuss, R_c is in the range of 1 to 10 k Ω . Because this is comparable with the quantized resistance of an ideal nanotube, one should keep in mind that absolute resistance values may be off by a factor ≈ 2 . In the next section we will come back to this point and report recent room-temperature resistance values.

Because we are reporting electric transport measurements for MWNTs, we would like to bring the differences and similarities between MWNTs and SWNTs to the reader’s attention. Since the electrical current of contacted MWNTs has been demonstrated to flow through the outermost carbon tube at low temperatures [10], experiments using MWNTs also address a single shell. The main difference is the diameter of the respective graphene cylinders. SWNTs have a typical diameter of $\approx 1\text{--}1.5$ nm whereas our MWNTs have diameters in the range 10–20 nm. This one order of magnitude difference in diameter relates to an order of magnitude difference in energy scale. For a semiconducting nanotube, tight-binding calculations predict a gap of order 0.1 eV for a 10-nm-diameter tube, whereas for a SWNT the gap is of order 1 eV [25]. This energy scale is also roughly valid for the energy separation between the first conduction and valence subbands above

and below the Fermi level for metallic tubes. Differences in electric resistance due to either semiconducting or metallic behavior are expected to be more pronounced for SWNTs because of the larger energy scale. In fact, these differences were observed with tunneling spectroscopy on SWNTs at low temperature [26].

If a SWNT is adsorbed on a substrate with metallic contacts, the nanotube has been found to closely follow the contour of the surface [27]. Because the metallic contacts have a finite thickness, the SWNT is strongly bent just at the edge of the contacts. These bending defects have been suggested to be one reason for the very high-ohmic contacts found in SWNTs contacted in this way [27]. This also suggests that all kinds of local deformations such as bends, kinks, and twist will cause some elastic backscattering, hence will destroy the exact quantization of the resistance valid for an ideal nanotube with transmission probability $t = 1$. Because all surfaces exhibit in general some roughness on the nm scale (except for atomically flat well-prepared substrates) it is hard to imagine that electric transport is ballistic for SWNTs adsorbed on a substrate. Here MWNTs (and also ropes of SWNTs) are advantageous, because the outer electrically measured tube is supported by 10–20 additional tubes inside which enhance the tube's rigidity. Computer simulations show that SWNTs may even collapse due to adhesive forces, whereas MWNTs are hardly deformed [28]. Furthermore, highly transparent contacts are presumably easier to achieve in case of MWNTs because the larger diameter results in a larger contact area for electric contact fingers of a given width [29].

There are other reasons which are in favor of MWNTs. Large-diameter carbon nanotubes have been predicted to have a larger mean-free path l_e for elastic scattering for a given defect density assuming a two-band tight-binding model with fluctuating diagonal and off-diagonal matrix elements [30]. The variance σ of these matrix elements describes the strength of the disorder. The mean-free path is found to be proportional to the diameter d as long as the subband separation is larger than the energy broadening due to scattering. This relates to the condition that $\sigma < C/\sqrt{d}$ where C is a constant.

As mentioned before, Frank et al. have suggested that transport in MWNTs is ballistic over micrometer distances even at room temperature. But in our opinion, no direct measurement of the elastic-scattering length exists for either MWNTs and SWNTs. Due to the high contact resistances, transport in SWNTs is largely dominated by single-electron tunneling effects [8,9]. Here, charge transport is dominated by the contacts and the Coulomb energy related to adding (removing) electrons to (from) the nanotube as a whole. Transport within the nanotube is of little significance for the externally measured resistance. Spectroscopy allows to access discrete $0d$ -states whose width can be used as a measure for the dephasing rate (but not for the rate of elastic scattering). Using this method, SWNTs have been demonstrated to be phase-coherent conductors over large distances $> 1 \mu\text{m}$ at low temperature $\lesssim 1 \text{ K}$ [8].

SWNTs have an additional disadvantage: their large curvature turns all nanotubes into semiconducting ones except for armchair nanotubes. This curvature effect can safely be neglected for MWNTs. In contrast, for MWNTs one may have to take a weak hybridization of electron states from neighboring tubes into account. Because of the different

diameters, the respective graphene lattices can never match up commensurately. Hybridization is therefore expected to be small. Note however, that in transport of MWNTs the energy landscape of an neighboring nanotube acts as a random potential. Taking an intertube overlap energy of 0.25 eV we estimate (based on the work of White and Todrov [30]) that l_e can still exceed $1 \mu\text{m}$ for nanotubes with a diameter of 30 nm.

With regard to electrical measurements in magnetic fields, orbital effects cannot be studied in SWNTs because extremely high magnetic fields would be required. In contrast, a magnetic field of 12 T is enough to induce a magnetic flux of $h/2e$ in a MWNT with outer diameter 15 nm. For this reason, valuable information can be obtained from magnetotransport experiments of MWNTs in parallel and perpendicular field. The Zeeman energy splitting due to the magnetic moment of the electrons can of course be observed both in single- and multi-wall nanotubes. From measurements of the Zeeman energy of SWNTs the gyromagnetic ratio g was found to be very close to the free electron value, i.e. $g = 2$ [8, 31]. Finally, the larger size of MWNTs (and SWNT ropes) facilitates their handling [32] and imaging by conventional scanning electron microscopy (SEM).

This brief advertisement for MWNTs should make clear that the structure and large diameter of MWNTs can be advantageous for the studying of certain electrical properties of carbon nanotubes. From a theoretical point of view, single-wall nanotubes are the model systems of choice. However, since MWNTs do behave as single tubes at low temperature, theories are equally well applicable to MWNTs.

A perfect metallic nanotube (also the large-diameter ones) has two $1d$ -subbands at the Fermi energy E_F originating from the π and π^* bands of graphene. The graphene bands intersect exactly at the corner points of the Brillouin zone, known as the K points. In the vicinity of these points the energy of the bands are given by $E(\mathbf{k}) = \pm \hbar v_F |\mathbf{k} - \mathbf{K}|$, where the Fermi velocity v_F is $\approx 10^6 \text{ m/s}$ [33]. Due to the two available subbands at E_F , nanotubes should ideally have a conductance of $G = 4e^2/h = 6.4 \text{ k}\Omega^{-1}$. No clear evidence for this universal (independent of size and wrapping) conductance for metallic tubes have been found to date. Frank et al. find values close to $2e^2/h$ and sometimes even some pre-plateaus at e^2/h [17]. There are also no systematic measurements on single nanotubes from which both the elastic l_e and the dephasing length l_ϕ can be extracted with the exception of the the pioneering work by Langer et al. [7].

This work intends to fill this gap. Values for l_e and l_ϕ have been deduced from measured interference effects such as weak localization (WL) and universal conductance fluctuations (UCF). We use conventional theories developed for diffusive transport appropriate for wires containing many conducting channels and discuss the shortcomings of this approach at the end.

Long-range Coulomb interaction of electrons in a one-dimensional wire (few conducting modes only) should strongly modify the Fermi-liquid picture of quasi-particles. An appropriate effective description is believed to be given by the Luttinger liquid (LL) model [5, 34, 35]. There is now striking evidence for LL-like behavior in SWNTs [36]. What about MWNTs? Can electron-electron interaction be accounted for by conventional Fermi liquid theory or do we have to use the LL-picture for MWNTs too?

1 Experimental techniques and results

1.1 Contacting single nanotubes

Single multi-wall carbon nanotubes (MWNTs) are contacted using conventional nanofabrication technology. A droplet of a dispersion of arc-produced nanotubes (NTs) in chloroform is used to spread the NTs onto a piece of thermally oxidized (400 nm) Si(100) substrate. Then, a PMMA resist layer is spun over the sample. An array of electrodes, each consisting of four contact fingers together with bonding pads, is exposed by electron-beam lithography. After development, a 120-nm Au film is thermally evaporated in a high-vacuum chamber. After lift-off, each structure of the array consists of four thin and narrow Au fingers ($\approx 100\text{--}200\text{ nm}$ in width) that end in bonding pads. We emphasize that no adhesion layer such as Cr or Ti has been used. This ensures that no magnetic impurities are introduced. The sample is now inspected by SEM and the structures that have one single nanotube lying below all four electrode fingers are selected for electric measurements. An example of a single MWNT contacted by four Au fingers with separation 350 nm (center to center) is shown in Fig. 1. Since the success of this contacting scheme works by chance, it is obvious that the yield is low. There are many structures that have either no or several NTs contacted in parallel. However, since a large array of more than 100 structures can readily be fabricated, this scheme has turned out to be very convenient. Alternatively, it is also possible to first structure a regular pattern of alignment marks on the substrate. After adsorbing the NTs, the sample is first imaged with SEM in order to locate suitable NTs. Having noted the coordinates aided by the marks, the electrodes can be structured directly onto the respective NTs with high precision. This improves the yield at the cost of an additional lithography step.

Let us emphasize that the Au electrodes are evaporated directly onto the nanotubes. Previously, we have been using the reverse scheme in which the electrode structures are made first and the NTs are adsorbed thereafter. In this latter scheme (nanotube over the contacts) the contact resistances were found to be large ($\gtrsim 1\text{ M}\Omega$). It was only with the aid of

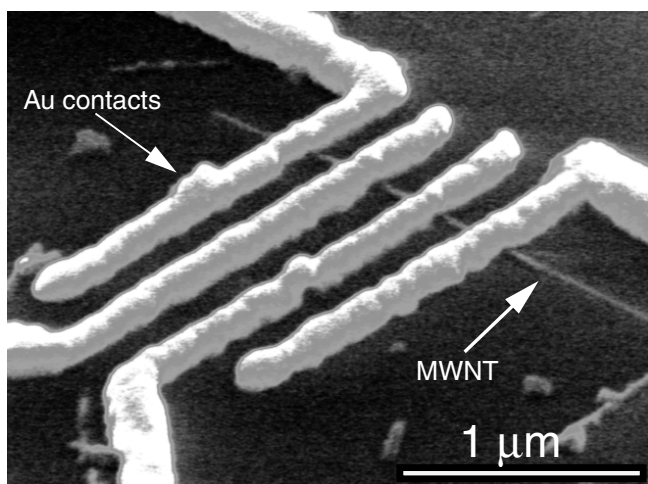


Fig. 1. Scanning electron microscopy image of a single multi-wall nanotube (MWNT) electrically contacted by four Au fingers from above. The separation between the contacts is 350 nm center to center

local electron exposure directly onto the NT–Au contacts that this resistance could be lowered to acceptable values [18]. In contrast, surprisingly low contact resistances ($\approx 5\text{ k}\Omega$) are obtained with the former scheme (nanotube under the contacts). It is also important to note that our Au–NT contacts are not long-term stable at room temperature. The contacts between Au fingers and NT are lost after a period of typically 1–2 weeks. Hence, it is important to measure the samples immediately after fabrication.

Only samples in which a single NT is contacted are selected for conventional equilibrium resistance measurements. An additional selection criterion based on contact resistances has been applied too: we require that all contact resistances are $\lesssim 10\text{ k}\Omega$ at room temperature. All NTs satisfying these selection criteria appear to be metallic, because the resistance is found to saturate in the limit of low temperatures. It is quite plausible that a semiconducting tube may never yield low-ohmic contacts due to the formation of a Schottky barrier. If this hypothesis is true we possibly throw away the semiconducting tubes and retain only the metallic ones for measurement. However, we are puzzled by the observation that of all contacted single NTs 80% have at least two low-ohmic contacts over which a two-terminal resistance $\lesssim 10\text{ k}\Omega$ is measured. Hence, one could conjecture that 80% of our MWNTs are apparently metallic. This contradicts the expectation that 2/3 of all NTs are semiconductors provided all diameters and chiralities are present with equal probability.

From a large number of MWNTs, each with four low-ohmic contacts, the average contact resistance is $3.8\text{ k}\Omega$ with a standard deviation of $5\text{ k}\Omega$ at room temperature (R_c ranges from $100\ \Omega$ to $20\text{ k}\Omega$). With our increase of experience in fabricating contacts, R_c could be lowered gradually. Our most recent batch shows values in the range of $100\ \Omega$ to $1\text{ k}\Omega$. In this limit of very low-ohmic contacts $R_{2t} \approx R_{4t}$, as expected for nearly ideal contacts. An ideal contact is defined to have no backscattering and to inject electrons in all modes equally. Electrons incident from the NT to the contact will then be adsorbed by the contact with unit probability. Because the contact couples to both right and left propagating modes equally, Ohm's law should be valid in this limit. It is important to realize that for ideal contacts R_{4t} cannot contain any nonlocal contribution, i.e. contribution to the resistance that arise from a NT segment not located in between the inner two contacts. Any sign of nonlocality points to the presence of non-ideal contacts.

Let us emphasize again the distinction between $R_c = (R_{2t} - R_{4t})/2$ and the quantized conductance of an ideal NT. Theoretically, the conductance of an ideal NT is quantized: $G = 4e^2/h$. The origin of this resistance can be traced back to the interface between the two-mode wire and the ideal macroscopic contact. In this respect it is purely a contact resistance [21]. This quantized resistance should not be confused with R_c . In the limit of an ideal NT with ideal contacts $R_c = 0$, but $R_{2t} = R_{4t} = h/4e^2$.

There are also samples which by chance have just one relatively high-ohmic contact, i.e. $R_c = 0.1\text{--}1\text{ M}\Omega$. Such samples are used for tunneling spectroscopy. The voltage-dependent differential conductance is measured on this contact. Because this contact resistance is 1 to 2 orders of magnitude higher than the resistance of the NT, most of the applied voltage drops locally at the contact. Such measurements give information on the local electron density of states

and are complementary to the transport experiments. It would be highly desirable to develop a scheme that allows the controlled fabrication of both low- and high-ohmic contacts to the same NT.

Finally, we mention that a single high-ohmic contact has occasionally been used as a gate electrode. However, the resistance of our metallic nanotubes could barely be modified by the gate voltage, indicating that Coulomb blockade is absent. This is presumably due to the other low-ohmic contacts that couple the NT strongly to the environment.

1.2 Temperature-dependent resistance

Four-terminal electrical resistances R have been measured as a function of temperature T in a He-3 system down to $T \approx 0.3$ K. The resistance always increases with decreasing temperature and saturates around 1–10 K. A typical example is shown in Fig. 2 (the dashed line corresponds to $h/2e^2 \approx 12.9$ k Ω). The increase from room temperature is moderate amounting to a factor $\lesssim 2-3$. This together with the low-temperature saturation is taken as evidence for the metallic nature of the MWNTs. Non-metallic behavior is characterized by a diverging resistance for $T \rightarrow 0$ as observed, for example, for semiconductors and in more exotic transport regimes such as variable range-hopping and strong localization. We emphasize that not only is the temperature dependence of $R(T)$ similar for all samples, but the absolute resistance values also fall into a relatively narrow range of $R_{4t} \approx 2-20$ k Ω , quite different from the original results of Ebbsen et al. [19].

The resistance increase at low temperatures is markedly different from what is known from (HOPG) graphite [37]. There, the resistivity decreases with decreasing temperature as commonly associated with metallic behavior. The decrease is caused by the suppression of electron–phonon scattering at low temperature. Although nanotubes are composed of the same graphene sheets, the $R(T)$ dependences are different. Where does this difference come from?

In trying to understand the temperature dependence of R , we first consider the simplest possible model. We will compare the absolute measured resistance values with an expression for the classical Drude resistance taking one graphene

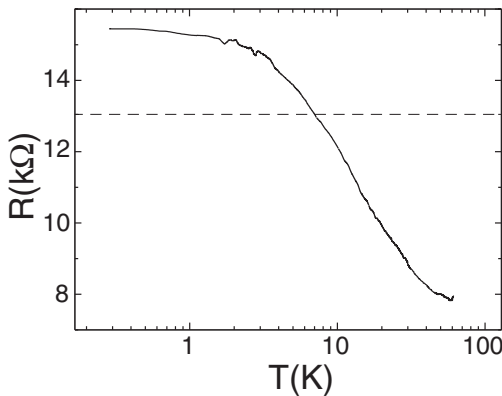


Fig. 2. Typical temperature-dependent electrical resistance $R(T)$ of a single MWNT measured in a four-probe configuration, i.e. the current is passed through the outer contacts and voltage is measured over the inner ones. The dashed line corresponds to the resistance quantum $h/2e^2$

cylinder and assuming 2d-diffusive transport, i.e. assuming $l_e \ll \pi d$. We thereby completely disregard the quantization of the wavevector around the tube circumference leading to 1d subbands. The electron states have energy $E = \pm \hbar v_F |\mathbf{k}|$, where \mathbf{k} is the 2d-wavevector measured with respect to the two independent Brillouin corner points. The Fermi energy is taken to be $E_F = 0$ and a reasonable value for the Fermi velocity $v_F = 10^6$ m/s is assumed [8, 33]. For the electron density of states (DOS) we obtain $n_{2d}(E) = 2E/\pi(\hbar v_F)^2$. Using the Einstein equation $\sigma_{2d} = e^2 n_{2d} D$, which relates the conductivity σ_{2d} to the diffusion coefficient $D = v_F l_e / 2$ and the electron density, the energy-dependent conductivity is found to be $\propto E$. To obtain the equilibrium sheet conductivity σ_{2d} at finite temperature the energy has to be replaced by kT . The equation now reads:

$$\sigma_{2d} \approx \left(\frac{2e^2}{h} \right) \frac{kT}{\hbar v_F} l_e \quad (1)$$

Due to the vanishing electron DOS for $E \rightarrow 0$, the resistance of a graphene sheet increases with decreasing temperature following $R(T) \propto T^{-1}$. Although a resistance increase is observed, the increase is not compatible with a T^{-1} dependence. Moreover, $R(T)$ saturates below ≈ 4 K. This saturation could be explained by a finite overlap with additional graphene cylinders giving rise to a narrow band of width Δ at the Fermi energy as in graphite. In the limit $kT < \Delta$ a constant DOS would develop. Now, kT has to be replaced by Δ in the above equation for σ_{2d} . Let us put in numbers in order to estimate the mean-free path l_e . Taking from the experiments $R = 10$ k Ω , contact separation $L = 350$ nm, tube diameter $d = 20$ nm and $\Delta = 4$ K (as suggested by the $R(T)$ saturation), we obtain $l_e \approx 13$ μ m. This large mean-free path violates the assumption that diffusion is 2-dimensional. Even more serious, $l_e \gg L$. The only way to reconcile this model with the requirement $l_e \lesssim L$ is to assume that a large number (30) of graphene cylinders carry the electric current equally. We know from the Aharonov–Bohm experiments that this is not the case [10]. We therefore conclude that the specific temperature dependence of R cannot be related to the energy-dependent DOS of graphene.

Within this simple Drude picture, the discrepancy can be resolved if we take into account the band-structure modifications imposed by the periodic-boundary condition along the circumference of the cylinder leading to 1d-subbands. In contrast to graphene, for which the DOS tends to zero for $E \rightarrow 0$, the DOS is constant in a relatively large energy window centered around the Fermi energy. This energy window is given by the subband separation ΔE_{sb} . Instead of the hypothetical and small hybridization energy, ΔE_{sb} should be inserted in the previous equation. With $\Delta E_{sb} = 100$ meV, typically valid for the outermost cylinders of our MWNTs, one arrives at a mean-free path of $l_e \approx 50$ nm, which is of order of the circumference of the tube. This number is of reasonable magnitude and in agreement with magnetoresistance measurement (see Sect. 1.4). This argument suggests that electron transport in MWNTs is not 2d-diffusive, but rather one-dimensional. Most importantly, it demonstrates that the 1d-subbands need to be considered in MWNTs as well.

The classical 1d-Drude resistance due to static disorder alone predicts a temperature-independent resistance. Temperature dependences can be caused by other scattering

mechanisms, such as electron–phonon and electron–electron scattering. In a first approximation we assume that electron–phonon scattering does not contribute significantly to momentum relaxation in carbon nanotubes. Since otherwise, $R(T)$ should decrease with decreasing temperature as observed for graphite. It is known however that electron–electron interaction can contribute significantly to R in nanoscaled devices at low temperature. In the limit of a piece of metallic wire that is weakly coupled to the environment, i.e. with $R_c \gg R_Q$ ($R_Q = h/2e^2 = 12.9 \text{ k}\Omega$ is the resistance quantum), Coulomb blockade turns the system into an insulating state [38]. This is the case, if $kT \ll E_c$, where $E_c = e^2/2C$ is the single-electron charging energy of the island (wire). The capacitance C' per unit length for our MWNTs is estimated from the expression of the geometric capacitance valid for an infinite conducting cylinder with diameter d supported above a conducting backplane at distance $a \gg d$:

$$C' = 2\pi\epsilon_0\epsilon_r (\ln(4a/d))^{-1}. \quad (2)$$

Taking $a = 400 \text{ nm}$ (thickness of the SiO_2), $\epsilon_r = 4.7$, a nanotube diameter of $d = 20 \text{ nm}$ with electric contacts spaced $L = 200 \text{ nm}$ apart (from edge to edge), the single-electron charging energy amounts to $E_c = 5 \text{ meV}$. Therefore, Coulomb blockade is expected to be relevant already for $T \lesssim 60 \text{ K}$. As one can see from Fig. 2 this indeed agrees with the onset of the resistance increase. It is therefore tempting to associate the resistance increase with charging effects (electron–electron interaction). True Coulomb blockade (CB), which would cause an exponential increase of R , is however not observed. We have also not found a significant gate effect characteristic for CB. We believe that this is due to the relatively low-ohmic contacts. In the opposite limit of a wire that is rather strongly coupled to the environment, CB theory predicts deviations from the classical conductance with moderate temperature and voltage dependences (power laws) [39]. In this limit it is not possible to separate the part that is charged from the environment. A unified treatment is needed. In case of a $1d$ -wire such a model is provided by the Luttinger-liquid (LL) theory [5, 34, 35]. Recently, zero-bias anomalies have been observed in SWNTs with power-law dependences in agreement with LL theory for nanotubes [36]. This experiment provides clear evidence that long-range Coulomb interaction can dominate the low-energy excitations of NTs. Because we observe similar anomalies (see Sect. 1.5) Coulomb interaction must be considered in order to understand $R(T)$ of MWNTs, too.

Summarizing this discussion, we have shown that the temperature dependence of the resistance cannot be related to the specific DOS of graphene. It is most likely caused by electron–electron interaction and (as will be shown) by interference contributions that are dominant at low temperature. This conclusion is supported by magnetoresistance measurements discussed below in Sect. 1.4.

1.3 Aharonov–Bohm oscillations in parallel field

The dependence of the electrical resistance of MWNTs in magnetic field has been studied both for parallel and perpendicular field. The parallel field case has recently been published [10]. For completeness we summarize the main results

in this section. Figure 3 shows a typical magnetoresistance (MR) measurement. On applying a field B the resistance decreases. This decrease is associated with the phenomenon of weak localization (WL) [40]. WL originates from the quantum-mechanical treatment of backscattering which contains interference terms adding up constructively in zero field. Backscattering is thereby enhanced leading to a resistance larger than the classical Drude resistance. Because the interference terms cancel in magnetic field of sufficient strength, WL results in a negative MR. However, for the specific geometry of a cylinder (or ring), the WL contribution is periodic in the magnetic flux through the cylinder with period $h/2e$ [41]. Indeed, in Fig. 3 the resistance has a second maximum at $B = 8.2 \text{ T}$. From this field a diameter of $d = 18 \text{ nm}$ is obtained for this MWNT. As was demonstrated by Bachtold et al. [10], the MR agrees with the Altshuler, Aronov, and Spivak (AAS) theory [42] only, if the current is assumed to flow through one or at most two metallic cylinders with a diameter corresponding to the measured outer diameter of the NT. It is therefore most likely that only one cylinder actually participates in transport. This may not be too surprising if we consider the strong anisotropy in conductivity for graphitized compounds and the fact that the electrodes are in direct contact with the outermost NT only. The conclusion that only *one* graphene cylinder carries the current can only unambiguously be drawn from the analysis of the low-temperature data ($T \lesssim 20 \text{ K}$). We emphasize that it is not possible to relate the resistance maxima at $\pm 8.2 \text{ T}$ to a magnetic flux of h/e , because a tube diameter would then result that is larger than the actually measured outer diameter. The observation of a pronounced $h/2e$ resistance peak proves that backscattering is present in our MWNTs. The NTs are therefore *not* ballistic.

In parallel magnetic field resistance maxima should occur periodically. Up to now, only the first period could be observed, which is little evidence for a periodic phenomenon. However, in Fig. 3 the onset of the second resistance peak is clearly seen. The resistance increases again at $14\text{--}15 \text{ T}$. The maximum is expected at $B = 16.4 \text{ T}$ (see arrows), which is unfortunately beyond the field range of our magnet.

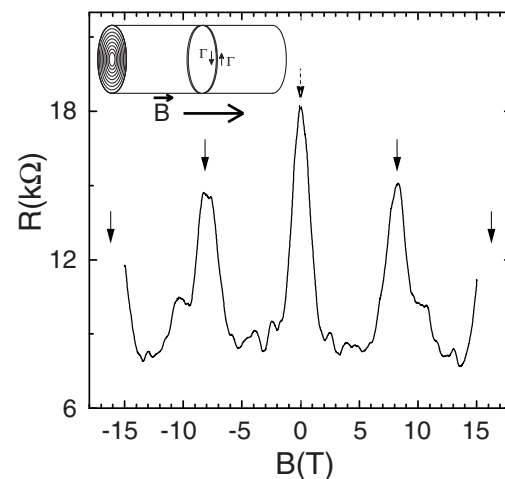


Fig. 3. Electrical resistance R as a function of magnetic field B of a MWNT aligned parallel to B . Arrows denote the resistance maxima corresponding to multiples of $h/2e$ in magnetic flux through the nanotube taking the outer diameter. The contact separation is 350 nm

We can use Fig. 3 to estimate the phase-coherence length. The zero-field resistance peak has a full width at half maximum of $2\Delta B \approx 2\text{ T}$. ΔB roughly corresponds to a flux quantum h/e within an area bounded by the wire diameter and the phase-coherence length l_ϕ . From this condition $l_\phi \approx 200\text{ nm}$ is obtained. As a test for consistency the WL correction to the conductance ΔG is compared with the measurement. For $1d$ -WL ΔG is of order $(2e^2/h)l_\phi/L$. Taking $L = 350\text{ nm}$ and $l_\phi = 200\text{ nm}$ we obtain $\Delta G = 4.4 \times 10^{-5}\text{ S}$, which is in very good agreement with the measured conductance change of $\Delta G = 4.6 \times 10^{-5}\text{ S}$. From MR measurements in perpendicular field similar coherence lengths are extracted. This will be discussed in the next section.

1.4 Interference effects in perpendicular field

Possible reasons for the measured resistance increase at low temperature (see Fig. 2) are interference corrections (WL) and electron–electron interaction effects. In order to quantify these contributions an extensive investigation of the magnetoresistance (MR) in perpendicular magnetic field was conducted. We note from the start that the conventional WL theory for diffusive transport is used in the analysis of our experiments [40].

We begin with a measurement that proves the presence of interference contributions. Figure 4 shows the four-terminal resistance of a MWNT measured at $T = 2.5\text{ K}$. Three distinct features can be seen: in the first place, the resistance is largest at $B = 0$. Second, there are aperiodic resistance fluctuations away from zero magnetic field, which are reproducible. And third, the MR is asymmetric in field, i.e. $R(-B) \neq R(B)$. All these features point to the presence of quantum interference. The resistance maximum at $B = 0$ is caused by weak localization as already mentioned in the previous section. The aperiodic fluctuations can be assigned to direct interference contributions and are known as universal-conductance fluctuations (UCF) [43]. These fluctuations depend on the specific scattering potential. They disappear if one would average over an ensemble of otherwise similar NTs. Particularly interesting is the third observation. By virtue of the reciprocity theorem [23] a two-terminal resistance must be symmetric in magnetic field. But a four-terminal resistance, such as the one measured in Fig. 4, may be asymmetric. The asymmetry arises if the voltage measured over the two inner contacts contains non-local contributions from parts of the wire that do

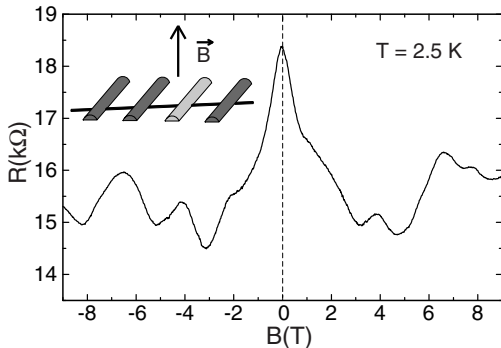


Fig. 4. Four-terminal magnetoresistance of a MWNT in perpendicular field measured at 2.5 K. The contact separation is 350 nm. The observed asymmetry is related to one of the voltage probes which was high-ohmic

not reside in between the two contacts over which the voltage is measured. For such non-local contributions to occur (a hallmark of mesoscopic physics [44]) two conditions need to be met: (i), the phase-coherence length should be large enough, and (ii), the voltage probes should not behave ideally in the sense that all electrons incident from the NT to the contacts are absorbed with probability one. Indeed, the contact resistance of one voltage probe was relatively high-ohmic for this sample. Its resistance was $\approx 150\text{ k}\Omega$, whereas the other contacts had $\lesssim 10\text{ k}\Omega$. When the temperature was increased above 20 K (not shown), the asymmetry as well as the aperiodic oscillations disappeared, whereas the resistance maximum at zero field remained present, although with lower magnitude. Exactly this dependence is expected once $l_\phi \ll L$.

The MR in Fig. 4 provides a convincing demonstration that quantum-mechanical interference terms strongly contribute to the electrical resistance of carbon nanotubes at low temperature. Let us emphasize that non-local contributions are prohibited if all contacts are low-ohmic (ideal). This is because electrons that arrive at the contacts are scattered with high probability into these where they are randomized. Hence, interference effects are terminated at ideal contacts. All MR measurements (also four-terminal ones) should therefore be symmetric in magnetic field. Any asymmetry is a signature of a ‘bad’ contact. Indeed, if all contacts are low-ohmic the resistance is found to be symmetric in B whether a 2-terminal or 4-terminal measurement is conducted.

An example is provided by Fig. 5 which shows the (4-terminal) MR of a MWNT for two temperatures (2.5 and 12 K). We mention that the two curves are not displayed vertically for clarity. This sample differs from the previous examples in the contact geometry. The two inner voltage contacts are now separated by $L = 1.9\text{ }\mu\text{m}$, instead of $L = 0.35\text{ }\mu\text{m}$ before. The MR of this NT has been measured for several temperatures and carefully analyzed in order to extract the phase-coherence length [45]. On applying a magnetic field the resistance again decreases in agreement with WL. Aperiodic fluctuations are superimposed and are assigned to UCF. The MR is compared to $1d$ -WL theory, i.e. $l_\phi > \pi d$. We note, that our measurements cannot be fitted by $2d$ or even $3d$

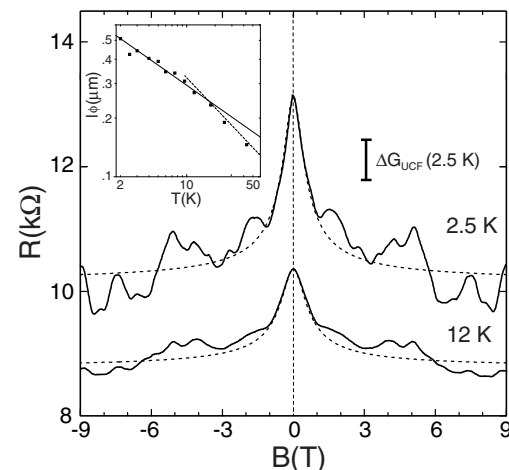


Fig. 5. Four-terminal magnetoresistance of a MWNT in perpendicular field for two temperatures. The voltage probes are separated by $1.9\text{ }\mu\text{m}$. Dashed curves show fits using one-dimensional weak-localization theory. Inset: deduced phase-coherence length l_ϕ as a function of temperature T

WL, which was found to describe the MR of NTs in previous work [6, 7, 46, 47]. The phase-coherence length l_ϕ is therefore larger than the diameter in our case ($d \approx 23$ nm for the NT of Fig. 5).

Phase randomization is caused by all kinds of inelastic scattering. At low temperature, however, electron–phonon scattering can be neglected and l_ϕ is determined by electron–electron interaction. Assuming diffusive transport, the phase-relaxation time τ_ϕ is related to l_ϕ by $l_\phi = (D\tau_\phi)^{1/2}$ where D is the diffusion coefficient. It has been pointed out that τ_ϕ has to be distinguished from the energy-relaxation time τ_{ee} due to electron–electron scattering [48]. The latter is determined by scattering processes that transfer energies of order kT , whereas the phase of the wavefunction can already be randomized by quasi-elastic scattering events with energy transfers $\ll kT$. For this reason $\tau_\phi < \tau_{ee}$ in general. The temperature range over which the last equation holds is particularly large in $1d$. At the lowest temperatures dephasing is always determined by quasi-elastic scattering. A cross-over occurs at $kT \approx \hbar/\tau_{ee}(T)$. Above this temperature the difference between τ_ϕ and τ_{ee} disappears. To compare the measurements with predictions, we use the $1d$ -WL theory which adequately takes dephasing by quasi-elastic scattering into account [48, 49]. The correction to the conductance ΔG for a wire of width w is given by:

$$\Delta G = -0.62 \frac{e^2}{\hbar L} \left(\frac{1}{l_\phi^2} + \frac{w^2}{3l_m^4} \right)^{-1/2}. \quad (3)$$

Here, $l_m(B)$ is the magnetic length given by $l_m^2 = \hbar/eB$. There are two important points to make: (i) our wire is not planar but actually a cylinder, so that $w = d$ cannot be assumed. (ii) the discussion in Sect. 1.2 has shown that the mean-free path for elastic scattering may be of order of the circumference of the NT. In this case flux cancellation due to intersecting closed electron trajectories has to be considered [50]. For these two reasons we treat the width w as an additional parameter (in addition to l_ϕ) and mention that w turns out to be $\approx d/2$. Best fits to theory are shown in Fig. 5 by dashed lines. A very good agreement is found. As a cross-check, UCF amplitudes deduced using l_ϕ agree with the observation. An example is given by the vertical bar in Fig. 5 which corresponds to the expected UCF amplitude at 2.5 K.

There are two other subtleties we would like to mention here. The equation for $1d$ -WL predicts a divergence for ΔG in the zero-temperature limit for which $l_\phi \rightarrow \infty$ is expected. However, this would only be true for an infinite long wire. The above equation is actually only valid if the length of the wire $\gg l_\phi$, because the localization correction saturates in the limit of $0d$ [51]. The second subtlety is due to the electric contacts which, if low-ohmic, limit the effective length of the wire due to dephasing. Once $l_\phi \approx L$ substantial dephasing will be caused by the contacts [48, 52]. Both cases predict a saturation of the resistance increase due to weak localization, as observed in $R(T)$.

Dephasing by the contacts can be incorporated in to the theory by taking the additional electromagnetic fluctuations of the external circuit into account. The equation for ΔG is thereby modified. In order to extract the ‘intrinsic’ l_ϕ from the measurements we have used such a modified $1d$ -WL equation [45].

The temperature-dependent coherence length is shown in the inset of Fig. 5. l_ϕ is of the order of a few 100 nm in agreement with the value obtained in the previous section using a qualitative argument. Below 10 K, l_ϕ scales with temperature according to $l_\phi \propto T^{-1/3}$ as expected from the theory which predicts

$$l_\phi = \left(\frac{DG_D L \hbar^2}{2e^2 kT} \right)^{1/3} \quad (4)$$

for dephasing by quasi-elastic electron–electron scattering [40, 53]. Here, G_D is the Drude conductance due to elastic scattering only. This equation allows us to extract the diffusion coefficient D from the magnitude of l_ϕ . We obtain $D = 450\text{--}900$ cm²/s. The large range is mainly due to errors in determining the Drude conductance. With a Fermi velocity of $v_F = 10^6$ m/s the elastic-scattering length is found to be $l_e = 90\text{--}180$ nm. l_e is indeed very large and the values are consistent with the estimate in Sect. 1.2 based on the absolute resistance value. Because $l_e \gtrsim \pi d$, transport in our MWNTs should be classified as *quasi-ballistic* [54] rather than diffusive. $l_\phi(T)$ only follows the $T^{-1/3}$ dependence up to 20 K. Above, l_ϕ decays faster, approximately as $\propto T^{-1/2}$. Two possibilities can account for this: (i) electron–phonon interaction may set in, or (ii) the transition to $\tau_\phi = \tau_{ee}$ may occur. Both scenarios are compatible with the observed temperature dependence within this limited temperature interval. Because there is no clear signature for electron–phonon scattering in the temperature dependence of the resistance for $T \leq 300$ K, we prefer the latter possibility. This is supported by the temperature (20 K) for which the transition occurs. Taking $D = 700$ cm²/s and $l_\phi(20\text{ K}) = 230$ nm gives a dephasing time of $\tau_\phi = 0.76$ ps corresponding to an energy uncertainty of ≈ 10 K in rough agreement with 20 K. Hence, for $T > 10\text{--}20$ K dephasing by quasi-elastic electron–electron scattering is no longer dominant because $\hbar/\tau_{ee} > kT$. There are not enough data points available to extract the temperature dependence of τ_{ee} . The dependence is also expected to change once l_e is no longer the shortest scattering length (clean limit). For the sake of the following consideration let us extrapolate l_ϕ to room temperature (RT) using the observed $T^{-1/2}$ dependence. We then obtain $l_\phi = 60$ nm at RT as an upper bound. It is therefore justifiable to say that MWNTs are not (quantum) ballistic at room temperature on a length scale of 1 μ m. There is substantial electron–electron scattering on a much shorter length scale. We believe that this conclusion is valid not only for our MWNTs but for all tubes of high quality for which scattering by static defects is not the dominant scattering mechanism at RT. Although l_{ee} is $\ll L$ at RT, its effect on the electric resistance is not obvious. If for example Umklapp processes are suppressed even at RT, electron–electron scattering does not change the resistance because the total momentum is conserved in the course of scattering. Hence, it may still be possible that the resistance is close to the expected quantized value.

Weak localization results in an increase of the electrical resistance at low temperatures. This is not the only contribution to the resistance increase, as can be seen from Fig. 5. For large magnetic field $\Delta G_{WL} \rightarrow 0$ but the resistance is still seen to be strongly temperature dependent. This temperature-dependent background resistance is usually associated with electron–electron interaction. While WL primarily enters as

a correction to the diffusion coefficient, the interaction suppresses the single-particle DOS. Furthermore, interaction effects are enhanced by disorder. For a diffusive wire for which the coherence length (the thermal length) is larger than the width but smaller than the length, theory predicts for the conductance correction $\Delta G_{\text{ee}} \propto T^{-1/2}$ [55]. Knowing $\Delta G_{\text{WL}}(T)$ one can plot $G(T) - \Delta G_{\text{WL}}(T)$ as a function of \sqrt{T} . Contrary to our expectation, the predicted temperature dependence is not observed. For this reason, $G(T)$ has been plotted in a log-log representation in Fig. 6. Filled symbols correspond to the measured conductance for zero field, whereas the open symbols represent the conductance after subtracting ΔG_{WL} . This plot is instructive. At low temperatures ($T \lesssim 4$ K) G saturates. In the range $4 \leq T \leq 40$ K the dependence follows approximately a power law $G \propto T^p$ with a small exponent $p \approx 0.1 - 0.2$. Unfortunately, no data points were measured between 50 K and RT. But the measured data points show a slight negative curvature around 10–40 K suggesting a possible saturation at high temperatures, which would come close to the expected conductance of a perfect NT, i.e. $4e^2/h$. This is – at least qualitatively – the $G(T)$ dependence expected for a Luttinger liquid with some degree of backscattering [56]. The exponent $p = 0.1 - 0.2$ is however relatively low and may indicate that the strong backscattering limit is not reached. Note, that for this sample the absolute value of G is surprisingly close to the quantized conductance $2G_0 = 4e^2/h$ expected for a perfect single-wall nanotube. That the actually measured room-temperature conductance is larger than $2G_0$ is not too surprising for the following two reasons: (i) at RT it is possible that additional graphene cylinders contribute to the measured conductance and not only the outermost shell, as inferred from Aharonov–Bohm measurements at low temperatures. (ii) even if we stick to just one single tube higher subbands have to be considered. The contribution to the conductance of a $1d$ -subband with a threshold energy E_1 is readily estimated to be $G_0 \exp(-E_1/kT)$. This has to be multiplied by the number of available subbands, which is four for the first higher (lower) subbands [57]. Hence, the total contribution to the conductance is $8G_0 \exp(-E_1/kT)$,

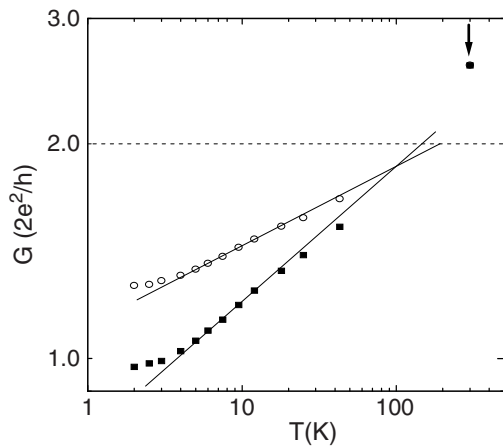


Fig. 6. Conductance G at zero magnetic field as a function of temperature T for the measurement shown in Fig. 5. Filled squares correspond to G at $B = 0$ and open circles to $G - \delta G_{\text{WL}}$ with δG_{WL} the contribution to the conductance from weak localization. The dashed horizontal line is the conductance expected for an ideal metallic carbon nanotube. The arrow points to the measured room temperature value

where E_1 is of order 50–60 meV. From this expression the conductance of a single 20-nm-diameter perfect nanotube is estimated to be rather $3G_0$ instead of $2G_0$ at RT.

1.5 Tunneling spectroscopy

Figure 7 shows a differential current–voltage characteristic (dI/dV) measured on a single MWNT using an inner contact which by chance was high-ohmic. This particular tunneling contact had $300 \text{ k}\Omega$ whereas the other contacts had resistances $\ll 10 \text{ k}\Omega$. The measured spectrum agrees surprisingly well with predicted spectra based on simple tight-binding calculations for a metallic NT [57, 58]. Firstly, there is a substantial DOS at the Fermi energy, i.e. at $V = 0$, so that the NT is metallic. Secondly, the almost symmetric peak structure, appearing as a pseudogap is caused by the additional $1d$ -subbands in the valence ($V < 0$) and conduction band ($V > 0$) with threshold energies of the order $\approx 50 \text{ meV}$. At the onset of the subbands van Hove singularities are expected. The spectrum in Fig. 7 agrees remarkably well with the scanning-tunneling measurements of Wildöer et al. for SWNTs [26]. But because of the difference in tube diameter the energy scales are different. Although the distance between the two first-order subbands ΔE_{sb} is found to $\Delta E_{\text{sb}} = 1.8 \text{ eV}$ for a SWNT with diameter $d = 1.3 \text{ nm}$, we found a smaller value of 0.12 eV . This is reasonable, since ΔE_{sb} should be proportional to d^{-1} [25, 58]. According to this relation, a diameter of 19 nm is predicted for our MWNT in good agreement with the measured outer diameter of $d = 17 \text{ nm}$. This is another independent proof of the conjecture that the electric contacts probe the outermost tube of a MWNT. Moreover, the observed occurrence of $1d$ -subbands in dI/dV shows that the motion of electrons in our NTs cannot be regarded as $2d$ -diffusive but must be ballistic on the scale of the tube diameter.

The van Hove singularities are broadened by thermal smearing as well as scattering. The limiting factor is scattering because $kT \ll \Delta E \approx 10 \text{ meV}$ for the measuring temperature which was $T = 4.2 \text{ K}$. An alternative estimate for

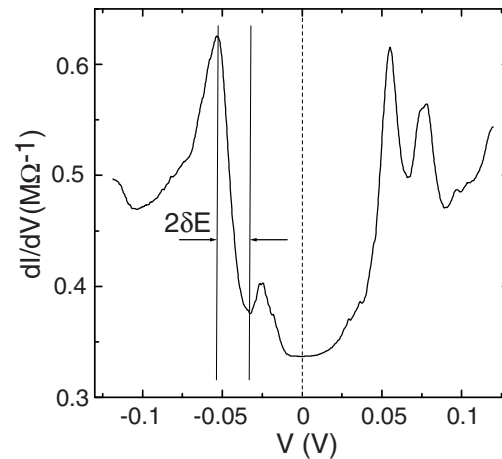


Fig. 7. Differential (tunneling) conductance dI/dV measured on a single MWNT using a high-ohmic contact ($300 \text{ k}\Omega$) at $T = 4.2 \text{ K}$. This spectra conforms to the DOS expected for a metallic nanotube in which the wavevector is quantized around the tube circumference leading to $1d$ -subbands. δE denotes the sharpness of the the observed van Hove singularities. Positive (negative) voltages correspond to empty (occupied) nanotube states

the scattering mean-free length can now be given. The $1d$ -subband can only develop as a pure eigenstate if $l_e \gg \pi d$. If we relate the scattering time to ΔE we obtain $l_e \lesssim 150$ nm. This relatively large elastic-scattering length supports the previous quantitative WL analysis which predicted similar lengths, i.e. $l_e = 90$ – 180 nm. These two consistent results convincingly establish that (our) MWNTs are quasi-ballistic conductors.

The observed spectrum in Fig. 7 nicely demonstrates that the peculiar band-structure effects of NTs are also found for MWNTs. We have to emphasize, however, that a spectrum with sharp van Hove singularities in close agreement with tight-binding calculations has only been observed on one sample until now, although several MWNTs have been studied. The prevailing spectra display a pronounced zero-bias anomaly on a smaller energy scale of 1–10 meV. For larger energies, they resemble Fig. 7 in the sense that a peak structure develops in dI/dV on the scale of the subband separation (0.1 eV) which may be associated with (broadened) van Hove singularities.

A typical zero-bias anomaly (ZBA) is shown in Fig. 8 for six temperatures ranging from 2–20 K. We note, that the full dI/dV displays a slight asymmetry in voltage and the data in Fig. 8 correspond to the symmetric part. A suppression of the tunneling DOS is expected for a strongly correlated electron gas [59]. Similar anomalies have recently been observed by Bockrath et al. for SWNTs [36]. Their measurement and analysis provide the first demonstration for Luttinger-liquid (LL) behavior in carbon NTs due to long-range Coulomb interactions. The LL theory describes the interaction with a single parameter g [59]. The non-interacting Fermi-liquid case corresponds to $g = 1$ and $0 < g < 1$ is valid for a LL with repulsive interaction. The parameter g is determined by the ratio of the single-electron charging energy to the single-particle level spacing and has been estimated to be $g = 0.2 - 0.3$ for SWNTs [35]. Because of the larger diameter of MWNTs, g may even approach a value of ≈ 0.35 for a single shell of diameter 30 nm. However, the exact value is difficult to estimate because the assumption of a single shell may be wrong in case of a MWNTs. Though contributing lit-

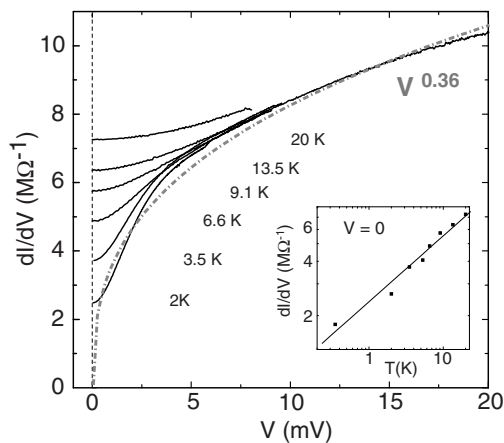


Fig. 8. Differential tunneling conductance dI/dV measured on a single MWNT at different temperatures T displaying a pronounced zero-bias anomaly on a relatively small voltage scale as compared to Fig. 7. *Inset:* log log representation of dI/dV vs. T for $V = 0$. The *dashed-dotted curve* displays the power-law $dI/dV \propto V^\alpha$ with $\alpha = 0.36$ deduced from the inset

tle to transport, the inner shells of a MWNT may strongly screen the long-range Coulomb interaction leading to $g \rightarrow 1$. It may be quite possible that the single-particle-like dI/dV spectrum of Fig. 7 is due to such a screening effect. Presumably, this is also the reason why a single particle like DOS has been measured on SWNTs in good contact to a Au substrate [26], although LL effects should be most prominent in unscreened SWNTs on an insulating substrate.

LL theory predicts power laws both for the voltage and temperature dependence, i.e. $dI/dV(T, V = 0) \propto T^\alpha$ and $dI/dV(T = \text{const}, V) \propto V^\alpha$ if $eV \gg kT$ [59]. The exponent α is related to g , explicitly $\alpha = (g^{-1} + g - 2)/8$ for tunneling into the bulk appropriate in our situation [35]. A power law with $\alpha \approx 0.36$ is deduced from $dI/dV(T, V = 0)$; see the inset of Fig. 8. For comparison with the observed dI/dV -voltage dependence, the dashed-dotted curve $\propto V^{0.36}$ has been plotted. The agreement with the measurements is not perfect, but taking into account the above-mentioned asymmetry quite satisfactory. The asymmetry is possibly caused by bandstructure effect. $\alpha = 0.36$ corresponds to $g = 0.21$. The same value was obtained by Bockrath et al. [36]. This exact agreement has presumably no significance because we use single MWNTs whereas they have used SWNT ropes. On the other hand, the agreement may indicate that the same physics is responsible for the ZBA. One has to keep in mind that the single-particle DOS can be suppressed for other reasons such as the presence of two-level and multi-level systems. However, we have not observed temporal fluctuations characteristic for such multi-level systems. Furthermore, the observed ZBA is not of magnetic origin, because we observe no significant change in a perpendicular magnetic field up to 12 T.

2 Critical discussion

Because resistivities were reported in previous studies using films of NTs we first like to make a comparison with these results. A typical value determined for the resistivity ρ is $10^{-3} \Omega\text{cm}$ [6, 47, 60]. Using the resistance that we have been measuring and the knowledge that the electric current flows through the outermost cylinder of the MWNT, we estimate $\rho \approx 10^{-6} \Omega\text{cm}$. This large difference indicates that the volume fraction of conducting NTs in thin-film samples is low. For this reason, it is not possible to compare the thin-film results with measurements on single NTs, because extrinsic effects (such as intertube hopping) most likely dominate the resistance of thin-film samples.

For all measured MWNTs we find a resistance of the order 10 k Ω at low temperature and a similar temperature dependence. The resistance increases by a factor $\approx 2 - 3$ if the temperature is lowered from RT to a few K. In addition, interference effects show up at low temperatures indicative of the presence of backscattering. In interpreting these results we have extensively used conventional weak-localization (WL) theory. This theory relies on diffusive transport in $2d$, i.e. l_e is implicitly assumed to be much smaller than the circumference of the NT. It may appear as a contradiction that using this theory l_e turns out to be larger than πd so that a central assumption for the validity of the theory is not met. In one example, tunneling spectroscopy has revealed a spectral density that agrees with band-structure calculations for which $l_e > \pi d$ is required. Furthermore, comparing the typically measured re-

sistance value with a Drude expression comparable values for l_e are found. These additional results give us confidence in the magnitude of l_e . MWNTs are therefore ballistic rather than diffusive. Strictly speaking, they are *quasi-ballistic*. However, we do not think that this conclusion contradicts the observed interference corrections, because interference effects have also been seen in split-gate quantum-point contacts (QPC) which are the prototype ballistic device [61]. In order to obtain the quantized conductance, theory assumes that the $1d$ -subbands in the constriction of the QPC are adiabatically coupled to states of the reservoirs on either side leading to zero backscattering [62]. In real devices perfect adiabaticity is never possible. Still, nice quantized conductance plateaus can be observed and the QPC appears to be ideal. However, if the temperature is lowered enough resonances appear in particular in the vicinity of subband thresholds. The conductance vs. gate dependence appears more and more ‘messy’ the lower the temperature. This is because of the increase in phase-coherence length which can lead to pronounced interference contributions in the resistance due to residual random potential fluctuations. Loosely speaking one may state that the QPC appears much more ideal at higher temperatures. The same may be true for NTs. Let us denote the mean fluctuation of the (self-consistent) potential by $\Delta E_d \approx \sqrt{\Delta^2 V}$. The appropriate energy scale with which to compare ΔE_d is the thermal energy kT [56]. If $kT \gg \Delta E_d$ scattering is weak and the system appears ideal. The conductance would be quantized if backscattering can be neglected all together. In contrast, if the temperature is lowered such that $kT < \Delta E_d$ the strong scattering regime is entered and resonances and the like are expected. Qualitatively, this is what we observe.

We note, that even at low temperature backscattering cannot be very strong. Based on the theoretically expected ideal conductance, the total transmission probability at low temperature is still reasonably large amounting to ≈ 0.5 . This has to be the case, because we have never observed a transition to strong localization. The source of the remaining scattering is not clear. The electric contacts are certainly not ideal, even if apparently low-ohmic. Scattering at the contacts alone is not sufficient to cause the aperiodic resistance fluctuations (UCF) seen at low temperatures. Therefore, there is some weak backscattering inherent to the MWNTs. This is also supported by comparing the resistances measured on one specific NT for different contact spacings. The resistance is larger for larger contact separations. The relatively large transmission probability and elastic-scattering length together with a disorder potential smaller than the subband separation (as suggested by Fig. 7) point to the high quality of the MWNTs that we are using.

Whereas the nanotubes are nearly ideal, the interference corrections (WL and AAS) can nicely be fitted by the traditional theories despite the fact that the theories are rigorously speaking no longer valid. The large range of (approximate) validity of the theory, which to us came as a surprise, is possibly just related to the the well-accepted universality of interference corrections both in magnitude and magnetic-field dependence. For the case of magnetoresistance in perpendicular field, we can imagine that the resistance corrections resemble weak localization even for few transport modes only. In contrast, for the parallel field case there is a serious problem. On the one hand, the AAS correction is based on time-reversed trajectories due to scattering along the circum-

ference of the tube, which requires $l_e \lesssim \pi d$. This is just the opposite of what we have inferred before. On the other hand, if we assume that the electronic structure has to be treated one-dimensionally, the band-structure is predicted to be periodically modulated with period h/e if the interior of a carbon NT is threaded by an Aharonov–Bohm flux [57, 63]. A metallic nanotube would be turned into a semiconducting one with a considerable band gap of the order 0.1 eV. Although the magnetotransport experiments in parallel field have been performed for much lower temperatures, a transition to an insulating state has never been observed [10]. This is puzzling, since dI/dV (Fig. 7) suggests that MWNTs can be described by the simple tight-binding band structure. This is a problem which deserves more attention in the future. Until now, magnetoresistance and dI/dV have been measured on different NTs. It would be highly desirable to obtain a complete set of data for one NT including dI/dV , $R(T)$, and MR in parallel and perpendicular field.

Finally, we like to mention another point which needs to be addressed by theory. For quantum wires fabricated from semiconducting heterostructures it is well known that backscattering is reduced if a perpendicular magnetic field of sufficient strength is applied [24]. In the limit of large fields, $1d$ -subbands are formed which are localized along the edges, so-called edge states [64]. Because modes at opposite edges propagate in different directions (are chiral) the suppression is very effective leading to the ideal quantization as observed in the integral quantum Hall effect. For NTs it has been shown that the wavefunctions of NTs are shifted to the sides in perpendicular magnetic field, so that edge states are formed [25]. In MWNTs this occurs already for a relatively low magnetic field of order 1 T, because the magnetic length $l_m = \sqrt{\hbar/eB}$ at 1 T is $l_m = 26$ nm and therefore comparable to the (outer) diameter of our MWNTs. We think it is important to theoretically study how the formation of edge states influences backscattering in the presence of weak disorder. A first treatment of this problem concludes that the MR should be positive [65], but this is not observed.

Similar to SWNTs, MWNTs are nearly ideal conductors with only two occupied $1d$ -subbands. Because the long-range Coulomb interaction is expected to be strong, the Luttinger-liquid (LL) picture is presumably the adequate description. This is supported by the observed zero-bias anomaly as well as the temperature-dependent conductance which cannot be accounted for by conventional Fermi-liquid theory. We think that MWNTs are LL with some degree of (weak) disorder. Assuming good (ideal) contacts, theory predicts $G \rightarrow 2G_0$ [56, 66] if $kT \gg \Delta E_d$ and $G \rightarrow 0$ in the opposite limit, provided the wire is infinitely long [56]. Since $\Delta E_d \approx kT$ at RT, $G \lesssim 2G_0$. Let us assume for the argument that $G = 2G_0$ at RT. This conductance corresponds to the two subbands at the Fermi energy. As has already been mentioned, the higher subbands also contribute to G at RT. Actually, one would rather expect to measure a conductance of $G \approx 3G_0$ instead of $2G_0$. Let us now look at the average room-temperature resistance values of recently measured MWNTs with very good contacts, i.e. $R_{2t} \approx R_{4t}$ to within 20%. For a contact separation of 350 nm we obtain $R_a = 3.2 \pm 1.6$ k Ω whereas $R_b = 9.6 \pm 2$ k Ω for a separation of 1.9 μm . Note, that there is a length dependence of the order 4 k $\Omega/\mu\text{m}$. Extrapolating these two values to zero contact separation gives $R(0) \approx 2$ k Ω corresponding to $6G_0$. This

is larger than $3G_0$ and suggests that more than one tube contributes to the conductance at RT. The most important remark we like to make here is concerned with the results of Frank et al. [17] who claim a universal conductance of G_0 for similar MWNTs at RT. This is definitely inconsistent with our observation. Because we find a nanotube conductance which is *larger* by a factor 6, our MWNTs cannot be blamed for being more dirty or more disordered. Actually, one may conclude the opposite. At present, we cannot offer a solution for this discrepancy.

To support ballistic transport over μm distances, Frank et al. came up with another interesting experimental observation. Large electric currents can be driven through MWNTs without destroying them. Based on the electric power and bulk heat conductivity for graphite the NT is expected to evaporate due to the large temperature rise. But this is not observed. This observation may however not be taken as a proof for ballistic transport. Rather it shows that dissipation is largely absent (which is an exciting fact by itself). We precisely know that our NT are *not* ballistic but still we are also able to pass large currents of similar magnitudes (mA) through our MWNTs. An interpretation of this phenomenon is difficult because it occurs in the non-linear transport regime for applied voltages much larger than the subband separation.

3 Conclusions

The reported study of electric transport of single MWNTs gives rise to results which appear to be in contradiction. For example, the observation of an Aharonov–Bohm effect with period $h/2e$ suggests diffusive transport on the scale of the circumference of the nanotube, i.e. $l_e \lesssim \pi d$. On the other hand, we have observed a dI/dV spectrum which agrees with tight-binding models assuming the existence $1d$ -subband. This just suggests the opposite, i.e. $l_e \gtrsim \pi d$. A large elastic-scattering length is also derived when comparing the measured resistance with a simple Drude-type equation. All our results can therefore be consistent only if l_e is of the order of the circumference; not very much larger, but also not very much smaller. Transport has therefore to be characterized as *quasi-ballistic*. What remains to be determined is the source of backscattering which at present is not known. Possible sources are static potential fluctuations due to adsorbates on the outer surface of the MWNT or potential variations caused by a partial wavefunction overlap between states of the outermost and next inner graphene cylinder.

There is a second ‘contradiction’ inherent to our presentation. On the one hand, we have extensively used theories such as weak-localization which are based on Fermi-liquid (FL) hypothesis. On the other hand, the observed suppression of the single-particle of states (the ZBA) suggests that NTs may develop a Luttinger-liquid (LL) state. It is quite uncomfortable to describe experiment A with FL theory and experiment B with LL theory. This is only justified because of a lack of theories that can be applied to analyze the measured data. If Luttinger-liquid is the correct description for NTs we need to know how the observed quantum interference corrections have to be described. Is there something similar to weak-localization in the LL picture? What happens in a magnetic field?

Acknowledgements. The nanotubes used in these works were kindly provided by L. Forró, J.-P. Salvetat, and J.-M. Bonard. In addition to the authors, the following persons contributed to this work: M. R. Buitelaar, A. Genkinger, and T. Nussbaumer. We have profited from inspiring recent discussions with P. Avouris, D. H. Cobden, W. A. de Heer, and E. Sukhorukov. This work has been supported by the Swiss National Science Foundation.

References

1. See for example: M.S. Dresselhaus, G. Dresselhaus, P.C. Eklund: *Science of Fullerenes and Carbon Nanotubes* (Academic Press, New York 1996); J.-C. Charlier, J.-P. Issi: *Appl. Phys. A* **67**, 79 (1998)
2. S.J. Tans, A.R.M. Verschueren, C. Dekker: *Nature* **393**, 49 (1998); see also: P.L. McEuen: *ibid.*, 15; R. Martel, T. Schmidt, H.R. Shea, T. Hertel, P. Avouris: *Appl. Phys. Lett.* **73**, 2447 (1998)
3. R. Saito, M. Fujita, G. Dresselhaus, M.S. Dresselhaus: *Appl. Phys. Lett.* **60**, 2204 (1992); J.W. Mintmire, B.I. Dunlap, C.T. White: *Phys. Rev. Lett.* **68**, 631 (1992); N. Hamada, S. Sawada, A. Oshiyama: *Phys. Rev. Lett.* **68**, 1579 (1992)
4. L. Balents M.P.A. Fisher: *Phys. Rev. B* **55**, R11973 (1997); Yu.A. Krotov, D.-H. Lee, S.G. Louie: *Phys. Rev. Lett.* **78**, 4245 (1997)
5. R. Egger A.O. Gogolin: *Phys. Rev. Lett.* **79**, 5082 (1997); C. Kane, L. Balents, M.P.A. Fisher: *Phys. Rev. Lett.* **79**, 5086 (1997)
6. S.N. Song, X.K. Wang, R.P.H. Chang, J.B. Ketterson: *Phys. Rev. Lett.* **72**, 697 (1994)
7. L. Langer et al.: *Phys. Rev. Lett.* **76**, 479 (1996)
8. S.J. Tans et al.: *Nature* **386**, 474 (1997)
9. M. Bockrath et al.: *Science* **275**, 1922 (1997)
10. A. Bachtold et al.: *Nature* **397**, 673 (1999)
11. A. Bachtold, C. Strunk, C. Schönberger, J.P. Salvetat, L. Forró: *Proceedings of the XIIth International Winter School on Electronic Properties of Novel Materials*, ed. by H. Kuzmany, J. Fink, M. Mehring, S. Roth (AIP, New York 1998) p. 65
12. A. Yu. Kasumov et al.: *Science* **248**, 1508 (1999)
13. H. Dai, E.W. Wong, C.M. Lieber: *Science* **272**, 523 (1996); A. Thess et al.: *Science* **273**, 483 (1996)
14. A.Y. Kasumov et al.: *Europhys. Lett.* **43**, 89 (1998)
15. P.J. Pablo et al.: *Appl. Phys. Lett.* **74**, 323 (1999); H.R. Shea, R. Martel, T. Hertel, T. Schmidt, Ph. Avouris: *Microelectron. Eng.* **46**, 101 (1999)
16. J. Kong, H.T. Soh, A.M. Cassell, C.F. Quate, H. Dai: *Nature* **395**, 878 (1998)
17. S. Frank, P. Poncharal, Z.L. Wang, W.A. de Heer: *Science* **280**, 1744 (1998)
18. A. Bachtold et al.: *Appl. Phys. Lett.* **73**, 274 (1998)
19. T.W. Ebbesen et al.: *Nature* **382**, 54 (1996)
20. J. Muster et al.: *J. Vac. Sci. Technol. B* **16**, 2796 (1998)
21. Y. Imry: In *Directions in Condensed Matter Physics*, ed. by G. Grinstein, G. Mazenko (World Scientific Press, Singapore 1986)
22. R. Landauer: *IBM J. Res. Dev.* **1**, 223 (1957); *ibid.* **32**, 306 (1988)
23. M. Büttiker: *IBM J. Res. Dev.* **32**, 317 (1988)
24. H. van Houten, C.W.J. Beenakker, B.J. van Wees: In *Semiconductors and Semimetals*, Vol. 35, ed. by M.A. Reed (Academic Press, New York 1992)
25. H. Aijki, T. Ando: *J. Phys. Soc. Jpn.* **62**, 1255 (1993)
26. J.W. G. Wildöer, L.C. Venema, A.G. Rinzler, R.E. Smalley, C. Dekker: *Nature* **391**, 59 (1998); T.W. Odom, J.-L. Huang, P. Kim, C. Lieber: *Nature* **391**, 62 (1998)
27. A. Bezryadin, A.R.M. Verschueren, S.J. Tans, C. Dekker: *Phys. Rev. Lett.* **80**, 4036 (1998)
28. T. Hertel, R.E. Walkup, Ph. Avouris: *Phys. Rev. B* **58**, 13870 (1998)
29. A. Rochefort, F. Lesage, D.R. Salahub, Ph. Avouris: *Cond. Mat/9904083*
30. C.T. White T.N. Todorov: *Nature* **393**, 240 (1998); M.P. Anantram T.R. Govindam: *Phys. Rev. B* **58**, 4882 (1998)
31. D.H. Cobden et al.: *Phys. Rev. Lett.* **81**, 681 (1998)
32. T. Hertel, R. Martel, P. Avouris: *J. Phys. Chem. B* **102**, 910 (1998)
33. P.R. Wallace: *Phys. Rev.* **71**, 622 (1947); G.S. Painter, D.E. Ellis: *Phys. Rev. B* **1**, 4747 (1970); D.P. DiVincenzo, E.J. Mele: *Phys. Rev.* **29**, 1685 (1984); J.W. Mintmire, D.H. Robertson, C.T. White: *J. Phys. Chem. Solids* **54**, 1835 (1993)
34. A. Komnik, R. Egger: *Phys. Rev. Lett.* **80**, 2881 (1998); A.A. Odintsov H. Yoshioka: *Phys. Rev. Lett.* **82**, 374 (1999)

35. R. Egger A.O. Gogolin: Eur. Phys. J. B **3**, 281 (1998)
36. M. Bockrath et al.: Nature **397**, 598 (1999)
37. See for example: M.S. Dresselhaus, G. Dresselhaus, K. Sugihara, I.L. Spain, H.A. Goldberg: In *Graphite Fibres and Filaments*, ed. by M Cardona, Springer Series in Material Science, Vol. 5 (Springer, Berlin, Heidelberg 1988)
38. H. Grabert, M.H. Devoret: *Single Charge Tunneling: Coulomb Blockade Phenomena in Nanostructures* (Plenum Press, New York 1992)
39. Yu.V. Nazarov: Pis'ma Zh. Eksp. Teor. Fiz. **49**, 105 (1989) [JETP Lett. **49**, 126 (1989)]; M.H. Devoret et al.: Phys. Rev. Lett. **64**, 1824 (1990); S.M. Girvin et al.: Phys. Rev. Lett. **64**, 3183 (1990); K.A. Matveev L.I. Glazman: Phys. Rev. Lett. **70**, 990 (1993)
40. See for example: G. Bergmann: Phys. Rep. **107**, 1 (1984); B.L. Altshuler, A.G. Aronov, M.E. Gershenson, Y.V. Sharvin: In *Soviet Scientific Reviews, Section A: Physics Reviews*, ed. by I.M. Khalatnikov (Harwood Academic, New York 1987); B.L. Altshuler P.A. Lee: Physics Today, Dec. issue, p. 36 (1988); A. Aronov: Physica Scripta T **49**, 28 (1993)
41. For a review, see: A.G. Aronov, Yu.V. Sharvin: Rev. Mod. Phys. **59**, 755 (1987)
42. B.L. Altshuler, A.G. Aronov, B.Z. Spivak: Pis'ma Zh. Eksp. Teor. Fiz. **33**, 101 (1981) [JETP Lett. **33**, 94 (1981)]
43. B.L. Altshuler: Pis'ma Zh. Eksp. Teor. Fiz. **41**, 530 (1985) [JETP Lett. **41**, 648 (1985)]; P.A. Lee, A.D. Stone: Phys. Rev. Lett. **55**, 1622 (1985); P.A. Lee, A.D. Stone, H. Fukuyama: Phys. Rev. B **35**, 1039 (1987)
44. For a review, see: R.A. Webb S. Washburn: Physics Today, Dec. issue, p. 46 (1988); C.P. Umbach, P. Santhanam, C. van Haesendonck, R.A. Webb: Appl. Phys. Lett. **50**, 1289 (1987)
45. A. Bachtold et al.: unpublished
46. M. Baxendale, V.Z. Mordkovich, S. Yoshimura, R.P.H. Chang: Phys. Rev. B **56**, 2161 (1997); A. Fujiwara et al.: *Proceedings of the International Winter School on Electronic Properties of Novel Materials 1997*, ed. by H. Kuzmany, J. Fink, M. Mehring, S. Roth, 65 (AIP, New York 1997)
47. G.T. Kim et al.: Phys. Rev. B **58**, 16064 (1998)
48. B.L. Altshuler, A.G. Aronov, D.E. Khmel'nitsky: J. Phys. C **15**, 7367 (1982)
49. P.M. Echternach, M.E. Gershenson, H.M. Bozler, A.L. Bogdanov, B. Nilsson: Phys. Rev. B **48**, R11 516 (1993); Y.B. Khavin, M.E. Gershenson, A.L. Bogdanov: Phys. Rev. Lett. **81**, 1066 (1998)
50. C.W.J. Beenakker, H. van Houten: Phys. Rev. B **38**, 3232 (1988)
51. U. Sivan, Y. Imry, A.G. Aronov: Europhys. Lett. **28**, 115 (1994); R.M. Clarke et al.: Phys. Rev. B **52**, 2656 (1995); B.L. Altshuler, Y. Gefen, A. Kamenev, L.S. Levitov: Phys. Rev. Lett. **78**, 2803 (1997); A.G. Huibers, M. Switkes, C.M. Marcus, K. Campman, A.C. Gossard: Phys. Rev. Lett. **81**, 200 (1998)
52. B.L. Altshuler, A.G. Aronov, A.Y. Zyuzin: Pis'ma Zh. Eksp. Teor. Fiz. **86**, 709 (1984) [JETP Lett. **59**, 415 (1984)]; K.K. Choi, D.C. Tsui, K. Alavi: Phys. Rev. B **36**, 7751 (1987)
53. B.L. Altshuler, A.G. Aronov, D.E. Khmel'nitsky: Solid State Commun. **39**, 619 (1981)
54. H. van Houten et al.: Acta Electronica **28**, 27 (1988)
55. P.A. Lee, T.V. Ramakrishnan: Rev. Mod. Phys. **57**, 287 (1985); B.L. Altshuler, A.G. Aronov: In *Electron-Electron Interactions in Disordered Systems*, ed. by M. Pollak A.L. Efros (North-Holland, Amsterdam 1984) pp. 1-153; H. Fukuyama: *ibid.* pp. 155-230
56. R. Egger, H. Grabert: Phys. Rev. B **58**, 10761 (1998)
57. W. Tian, S. Datta: Phys. Rev. B **49**, 5097 (1994)
58. C.T. White, J.W. Mintmire: Nature **394**, 29 (1998); J.W. Mintmire, C.T. White: Phys. Rev. Lett. **81**, 2506 (1998).
59. For a review see: M.P.A. Fisher, L. Glazman: In *Mesoscopic Electron Transport*, ed. by L.L. Sohn, L.P. Kouwenhoven, G. Schön, NATO ASI Series E: Appl. Sci. **345** (Kluwer Academic, Dordrecht 1997)
60. G. Baumgartner et al.: Phys. Rev. B **55**, 6704 (1997); J.E. Fischer et al.: Phys. Rev. B **55**, R4921 (1997)
61. G. Timp et al.: Phys. Rev. Lett. **59**, 732 (1987); A. Szafer, A.D. Stone: Phys. Rev. Lett. **62**, 300 (1989)
62. L.I. Glazman, G.B. Lesovik, D.E. Khmel'nitsky, R.I. Shekhter: Pis'ma Zh. Eksp. Teor. Fiz. **48**, 218 (1988) [JETP Lett. **48**, 238 (1988)]; A. Yacoby, Y. Imry: Phys. Rev. B **41**, 5341 (1990)
63. H. Aijiki, T. Ando: Physics B **201**, 349 (1994)
64. B.I. Halperin: Phys. Rev. B **25**, 2185 (1982); A.H. MacDonald, P. Streda: Phys. Rev. B **29**, 1616 (1984); for a review, see: M. Büttiker: In *Semiconductors and Semimetals*, Vol. 35, ed. by M.A. Reed (Academic Press, New York, 1992)
65. T. Ando, T. Nakanishi: J. Phys. Soc. Jpn. **67**, 1704 (1998)
66. D.L. Maslov, M. Stone: Phys. Rev. B **52**, R5539 (1995)